

Repopulation of Murine Kupffer Cells after Intravenous Administration of Liposome-Encapsulated Dichloromethylene Diphosphonate

Takashi Yamamoto,^{*†} Makoto Naito,^{*†}
Hiroshi Moriyama,^{*†} Hajime Umezu,^{*†}
Hirotami Matsuo,[‡] Hiroshi Kiwada,[‡] and
Masaaki Arakawa[†]

From the Second Department of Pathology* and the Second Department of Internal Medicine,[†] Niigata University School of Medicine, Niigata, and the Faculty of Pharmaceutical Sciences,[‡] University of Tokushima, Tokushima, Japan

Kupffer cells were selectively eliminated in mice by the intravenous administration of liposome-entrapped dichloromethylene diphosphonate. At 5 days, small peroxidase-negative and acid-phosphatase-weakly-positive macrophages appeared, increased in number, and differentiated into peroxidase- and acid-phosphatase-positive Kupffer cells. Repopulating small macrophages actively proliferated, and the number of Kupffer cells returned to the normal level by day 14. The numbers of macrophage precursors in the liver as detected by the monoclonal antibodies ER-MP20 and ER-MP58 increased after liposome-entrapped dichloromethylene diphosphonate injection. ER-MP58-positive cells proliferated and differentiated into ER-MP20-positive cells and eventually into BM8-positive Kupffer cells in the liver. Bone-marrow-derived ER-MP58-positive cells were also detectable in the liver and differentiated into ER-MP20-positive cells, but they did not become BM8-positive macrophages. Macrophage colony-stimulating factor mRNA expression was enhanced in the liver 1 day after injection. The administration of macrophage colony-stimulating factor did not shorten the period of Kupffer cell depletion but increased the number and the proliferative capacity of repopulating Kupffer cells. These findings implied that repopulating Kupffer cells are derived from a macrophage precursor pool in the liver rather than from bone-marrow-derived monocytes. Local production

of macrophage colony-stimulating factor in the liver plays a crucial role in the differentiation, maturation, and proliferation of Kupffer cells. (Am J Pathol 1996, 149:1271-1286)

According to the concept of the mononuclear phagocyte system, Kupffer cells constitute a short-lived and nondividing population and are supplied by a high rate of monocyte influx to the liver.¹ The mean turnover time of Kupffer cells is estimated at 3.8 days in mice¹ and 12.6 days in rats.² However, the proliferative potential of Kupffer cells has been confirmed by partial hepatectomy,³⁻⁶ the administration of various macrophage stimulants,^{4,7} and parabiosis,^{8,9} indicating that Kupffer cells are self-renewing. In our studies of mice rendered severely monocytopenic by the administration of ⁸⁹Sr^{10,11} we found that Kupffer cells can survive without an influx of monocytes. Thus, the differentiation and proliferation kinetics of Kupffer cells has not been completely settled.

Various approaches have been followed to analyze macrophage kinetics. Liposome-encapsulated dichloromethylene diphosphonate (MDP), which is highly cytotoxic to macrophages, is a useful tool with which to examine repopulating macrophages in several tissues. Using this method, Rooijen et al¹²⁻¹⁷ have depleted tissue macrophages and studied their repopulation. However, the kinetics of repopulating Kupffer cells and their precursor cells have not been investigated.

Among several macrophage growth factors, macrophage colony-stimulating factor (M-CSF) plays an important role in the development, differentiation, proliferation, and function of macrophages.¹⁸⁻²¹ In

Supported by grants-in-aid for scientific research from the Ministry of Education, Science, and Culture of Japan (07670235).

Accepted for publication June 11, 1996.

Address reprint requests to Dr. Makoto Naito, Second Department of Pathology, Niigata University School of Medicine, Asahimachi-dori 1, Niigata 951 Japan.

op/op mice,^{19,20} macrophage differentiation is defective because of the complete absence of functional M-CSF. The number of Kupffer cells in op/op mice was reduced to 30% of that of normal littermates, and their ultrastructure was small and immature. M-CSF corrects the numerical and morphological defects of Kupffer cells in mutant mice.¹⁹ These observations indicate that M-CSF is a key molecule for the development and differentiation of Kupffer cells. Because fetal and adult livers produce M-CSF,^{22,23} the liver may provide a microenvironment for Kupffer cell differentiation by the local production of M-CSF.

In this study, we performed immunohistochemical, ultrastructural, and autoradiographic studies on murine Kupffer cells and their precursors after a single intravenous injection of liposome-entrapped MDP, to clarify the repopulation mechanism of Kupffer cells. The role of M-CSF in the repopulation of Kupffer cells was also investigated by examining the expression of M-CSF mRNA in the liver and by injecting M-CSF into Kupffer-cell-depleted mice.

Materials and Methods

Preparation of Liposome-Entrapped MDP

Multilamellar liposomes were prepared as described.²⁴ In brief, 58.72 mg of phosphatidylcholine (Nihon Seika, Hyogo, Japan), 8.75 mg of dehexadecyl phosphate, and 24.75 mg of cholesterol (Wako, Tokyo, Japan) were dissolved in chloroform in a round-bottom flask and dried under reduced pressure. The lipids were then hydrated in 5 ml of phosphate-buffered saline (PBS) containing 650 mmol/L (0.9455 g) MDP and vortex mixed at room temperature. The liposomes were extruded through polycarbonate membranes (Costar Corp., Pleasanton, CA) with a pore size of 0.8 μm . Non-encapsulated MDP was removed by ultracentrifugation. The liposomes were composed of phosphatidylcholine/dehexadecyl phosphate/cholesterol at a molar ratio of 5:1:4.

Animals

BALB/c mice were purchased from Charles River Japan (Tokyo, Japan) and maintained under routine conditions at the Laboratory Animal Center of Niigata University School of Medicine. Eight-week-old male mice were intravenously injected with 0.1 ml of liposome-entrapped MDP. The liver, bone marrow cells, and peripheral blood cells were removed at various intervals after MDP-liposome injection. At various time points, three mice were killed by ether anesthe-

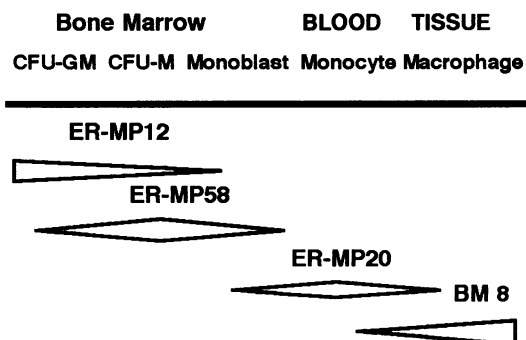


Figure 1. The monoclonal antibodies used in this study recognize antigens on macrophages and their precursors. BM8 recognizes mature tissue macrophages. ER-MP20 recognized immature macrophages, monocytes, and promonocytes. ER-MP58 recognized cells from colony forming units of granulocytes and macrophages (CFU-GM) to monoblasts. ER-MP12 recognized mainly blastic cells as well as a few promonocytes.

sia. Mice given liposome-entrapped MDP and subcutaneously injected with 5 μg of recombinant human M-CSF (Morinaga Milk Co., Tokyo, Japan) daily from 2 days after liposome-entrapped MDP injection were also examined.

Blood Cell Count

A small amount of blood was sampled from the tail vein of each animal, and the number of white blood cells was calculated. On a blood film, 1000 white blood cells were differentially counted.

Monoclonal Antibodies

The monoclonal antibodies BM8, ER-MP12, ER-MP58, and ER-MP20 (BMA Biomedicals, Augst, Switzerland) were used at a dilution of 1:100. These monoclonal antibodies recognize antigens on macrophages and their precursors at different stages of differentiation (Figure 1).^{25,26}

Immunohistochemistry

The liver was fixed for 4 hours at 4°C in periodate-lysine-paraformaldehyde (PLP), washed for 4 hours with PBS containing 10, 15, and 20% sucrose, embedded in OCT compound (Miles, Elkhart, IN), frozen in dry ice/acetone, and cut by a cryostat (Bright, Huntington, UK) into 6- μm -thick sections. Cytospin specimens of bone marrow cells and peripheral blood smears were fixed in acetone for 5 minutes. After inhibition of endogenous peroxidase activity by the method of Isobe et al,²⁷ we performed immunohistochemistry using the anti-mouse macrophage monoclonal antibody BM8 and anti-mouse monoclo-

nal antibodies ER-MP12, ER-MP20, and ER-MP58 against macrophage precursors.^{25,26} As a secondary antibody, we used anti-rat Ig-horseradish-peroxidase-linked F(ab')₂ fragment (Amersham, Little Chalfont, UK). After visualization with 3,3'-diaminobenzidine (Dojin Chemical Co., Kumamoto, Japan), nuclear staining with methylene green, and mounting with resin, the positive cells with nuclei per 1 mm² were counted using a light microscope.

Immunohistochemical Double Staining

Immunohistochemical double staining with ER-MP58, ER-MP20, and BM8 was performed as described previously²⁸ with minor modification. In brief, after inhibiting endogenous peroxidase activity as described by Isobe et al,²⁷ cryostat sections were incubated with the first primary monoclonal antibody. After incubation with anti-rat Ig-horseradish-peroxidase-linked F(ab')₂ fragment, the reaction was stained brown with diaminobenzidine. The sections were washed twice with glycine/HCl buffer for 1 hour and then incubated with the second primary monoclonal antibody. After incubation with anti-rat Ig-horseradish-peroxidase-linked F(ab')₂ fragment, they were incubated with 4-chloro-1-naphthol and processed as above to stain positive cells blue. As for the negative control, primary antibodies were replaced by nonspecific rat serum.

Immunofluorescent Microscopy

Liver sections prepared by the method described above were stained by an indirect method using the anti-macrophage and anti-macrophage precursor monoclonal antibodies mentioned above. As a secondary antibody we used fluorescein-isothiocyanate-labeled anti-rat Igs (Dako, Carpinteria, CA). Double staining with ER-MP20 and BM8 was performed by using anti-rat Ig-horseradish-peroxidase-linked F(ab')₂ fragment followed by incubation in 0.1 mol/L glycine/HCl buffer (pH 2.2) to remove the reacted primary antibody and then fluorescein-isothiocyanate-labeled anti-rat IgG, respectively. BM8 positivity is observed as a diaminobenzidine reaction under the microscope, and ER-MP20 positivity is observed by fluorescence microscopy.

Acid Phosphatase Cytochemistry

To demonstrate acid phosphatase activity, the livers were fixed with PLP solution as described above, frozen, and cut into sections. Sections were stained as described previously²⁹ with minor modification.

Sections were incubated in the medium containing 50 ml of acetate buffer, pH 5.0, 10 mg of naphthol-AS-BI phosphate (Sigma Chemical Co, St. Louis, MO) in 0.5 ml of ethylene glycol monomethyl ether (Sigma Chemical Co, St. Louis, MO), and 2 ml of freshly prepared hexazotized pararosaniline (Sigma). Positive cells were stained red.

Ultrastructural Peroxidase Cytochemistry

To cytochemically demonstrate peroxidase activity, the liver was perfused with 1.5% glutaraldehyde through the portal vein for 1 minute as described by Wisse.³⁰ After washing in 0.05 mol/L cacodylate buffer, the tissues were chopped into 50- μ m-thick sections using a vibratome (Lancer, St. Louis, MO) and then incubated according to Graham and Karnovsky.³¹ Ultrathin sections were observed under a Hitachi H-800 electron microscope (Hitachi, Tokyo, Japan) after staining with lead citrate.

Autoradiography with [³H]Thymidine

We purchased [³H]thymidine (specific activity, 3.0 TBq/mmol) from DuPont (Wilmington, DE) and stored it at 4°C. The time of injection of [³H]thymidine was varied with respect to when the injection of liposome-entrapped MDP was given. Three groups of experiments were performed. In the first group, mice were intravenously injected with 1 MBq of [³H]thymidine for 60 minutes at 1, 2, 3, 5, 7, 10, 14, 21, and 28 days after liposome-entrapped MDP injection and then killed, and the liver, peripheral blood, and bone marrow cells were removed. After immunohistochemical staining with ER-MP12, ER-MP20, ER-MP58, and BM8, slides were dipped into a Sakura NR-M2 liquid emulsion (Konica, Tokyo, Japan) diluted 1:2 with water, exposed for 2 weeks at 4°C, and developed. Cells with 10 or more grains in the nucleus above background were considered as labeled.

In the second group, we injected the mice with 0.1 ml of liposome-encapsulated MDP immediately after injecting 1 MBq of [³H]thymidine. At 1, 2, and 3 hours and at 7 days, three mice were sacrificed. In the third group, 1 MBq of [³H]thymidine was intravenously injected at 2 days after giving mice a liposome-entrapped MDP injection. At 2, 3, 5, 7, 10, 14, 21, and 28 days after liposome-entrapped MDP injection, the mice were sacrificed and examined as described above.

Table 1. *Oligonucleotides Used*

mRNA	Primers	Sequences (5' to 3')	Products (bp)
M-CSF	Sense	GAGGATCCTGTTTGCTACCTA	187
	Antisense	GTTGAGCTCCTCATAAGTCCTGG	
GM-CSF	Sense	GAAACGGACTGTGAAACACA	230
	Antisense	CTGTGGCTGTGCCACATCTC	
IL-3	Sense	GAAGTGGATCCTGAGGACAGATACG	292
	Antisense	GACCATGGGCCATGAGGAACATTC	
IL-1 α	Sense	CTCTAGAGCACCATGCTACAGAC	288
	Antisense	GACCATGGGCCATGAGGAACATTC	
β -actin	Sense	TGGAATCCTGTGGCATCCATGAAAC	348
	Antisense	TAAACGCAGCTCAGTAACAGTCCG	

RNA Isolation and mRNA Analysis by Reverse Transcriptase Polymerase Chain Reaction (RT-PCR)

Total cellular RNA was isolated from the liver of each mouse by phenol-chloroform extraction.³² In brief, at 2, 6, and 12 hours and at 1, 2, 3, and 5 days after liposome-entrapped MDP injection, the liver was removed and homogenized at room temperature in 5 ml of solution D (4 mol/L guanidinium isothiocyanate, 0.5% *N*-lauroylsarcosine, 25 mmol/L sodium citrate, 100 mmol/L 2-mercaptoethanol) in a glass Teflon homogenizer and transferred to a 12-ml polypropylene tube. Subsequently, 0.4 ml of 2 mol/L sodium acetate (pH 4), 4 ml of water-saturated phenol, and 0.8 ml of chloroform/isoamyl alcohol was added to the homogenate. After centrifugation, the aqueous phase was transferred to a fresh tube, mixed with 2 ml of isopropanol, and placed at -20°C overnight to precipitate RNA. After sedimentation, the RNA pellet was dissolved in 2 ml of solution D and precipitated with 2 ml of isopropanol. The RNA yield was determined by the A260, and the purity of the RNA was assessed on the basis of the A260/A280 ratio with a nucleic acid spectrometer (GeneQuant, Pharmacia, Uppsala, Sweden). A 2- μg amount of total RNA was mixed with 4 μl of RT buffer, 2 μl of 0.1 mol/L dithiothreitol, 0.5 μl of RNAsin (Promega, Madison, WI), 1 μl of 10 mmol/L dNTPs (Pharmacia), 2 μl of random primer (Pharmacia), 0.5 μl of RT (Gibco, Gaithersburg, MD), and distilled water to bring the final volume to 20 μl , and the mixture was incubated at 42°C for 60 minutes and then boiled at 95°C for 3 minutes. PCR amplification was performed by using a TP cycler-100 (Toyobo, Osaka, Japan). The reaction mixture consisted of 5 μl of sample cDNA, 5 μl of PCR amplification buffer, 2 μl of 25 mmol/L MgCl_2 , 4 μl of 2.5 mmol/L dNTPs, 0.3 μl of *Taq* DNA polymerase (5 U/ μl ; Promega), 2 μl of 20 mmol/L primer, and 29.7 μl of double-distilled water to bring the final volume to 50 μl . All of the PCR primers were made to order by Kurabo Biomedicals (Osaka, Japan). The

oligonucleotides used are shown in Table 1. The predicted sizes of amplified products for M-CSF, granulocyte/macrophage (GM)-CSF, interleukin (IL)-3, IL-1 α , and β -actin were 187, 230, 292, 288, and 348 bp, respectively. The mixture was first incubated for 5 minutes at 95°C and then cycled 30 times at 95°C for 1 minute, 57°C for 2 minutes, and 72°C for 2 minutes and elongated at 72°C for 10 minutes. The samples were separated on a 1.5% low-melting-point agarose gel containing 0.3 $\mu\text{g/ml}$ (0.003%) of ethidium bromide, and bands were visualized and photographed using ultraviolet transillumination. For further analysis, livers removed at 24 hours after injection with liposome-entrapped MDP were removed and divided into the mononuclear cell (MNC) fraction and the liver cell fraction as described.³³ Briefly, the liver was cut into small pieces with scissors, pressed through a 100-gauge stainless steel mesh, and suspended in RPMI 1640 medium supplemented with 5% heat-inactivated fetal calf serum. MNCs were isolated from parenchymal hepatocytes by Ficoll-Isopaque (specific gravity: 1.090) gradient centrifugation. RNA was extracted from both cell fractions and examined as described above.

Statistics

The significance of the data was evaluated by Student's *t*-test.

Results

Changes in Numbers of White Blood Cells and Monocytes in Peripheral Blood of Mice after Liposome-Entrapped MDP Injection

In mice injected with liposome-entrapped MDP, the white blood cell count increased from 8,000 to 50,000 per mm^3 , and the number of monocytes in the peripheral blood also rapidly increased in parallel. The numbers of neutrophils and monocytes in the

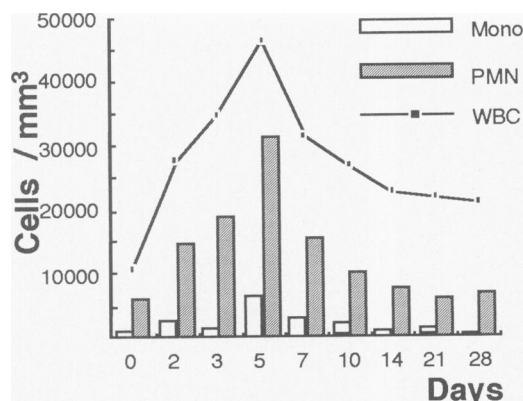


Figure 2. Changes in the numbers of white blood cells (WBC), neutrophils (PMN), and monocytes (Mono) after administration of liposome-entrapped MDP.

MDP-treated mice increased nearly fivefold within 5 days. At 2 days after injection, the number of neutrophils had more than doubled. Monocytes constituted 6 to 12% of the total white blood cell count from 2 to 10 days after injection, and the number of these cells remarkably increased to 7500/mm³ at day 5 (Figure 2).

Depletion and Repopulation of Kupffer Cells in Liposome-Entrapped MDP-Treated Mice

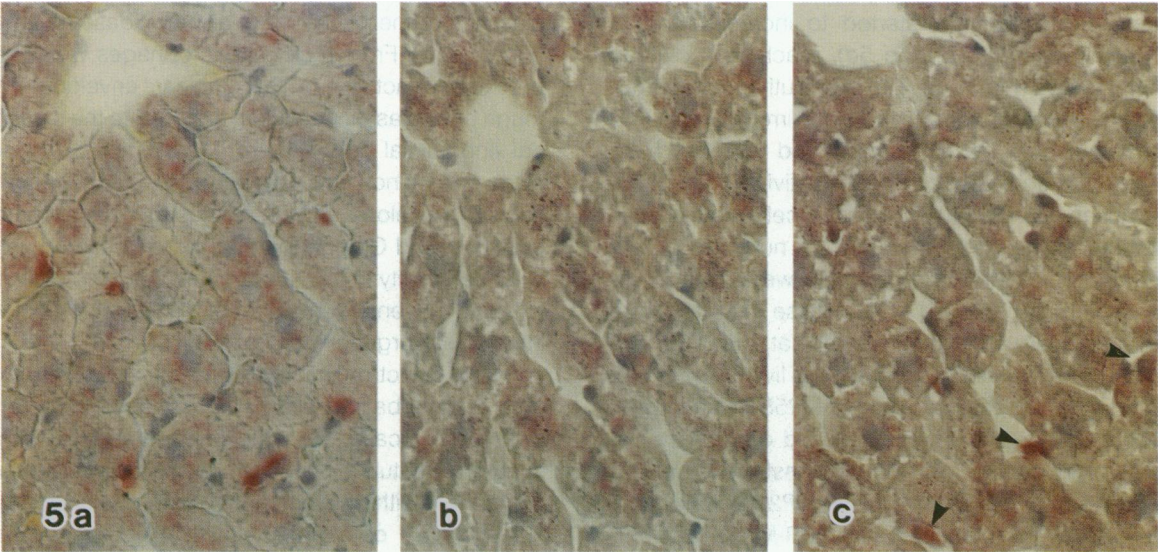
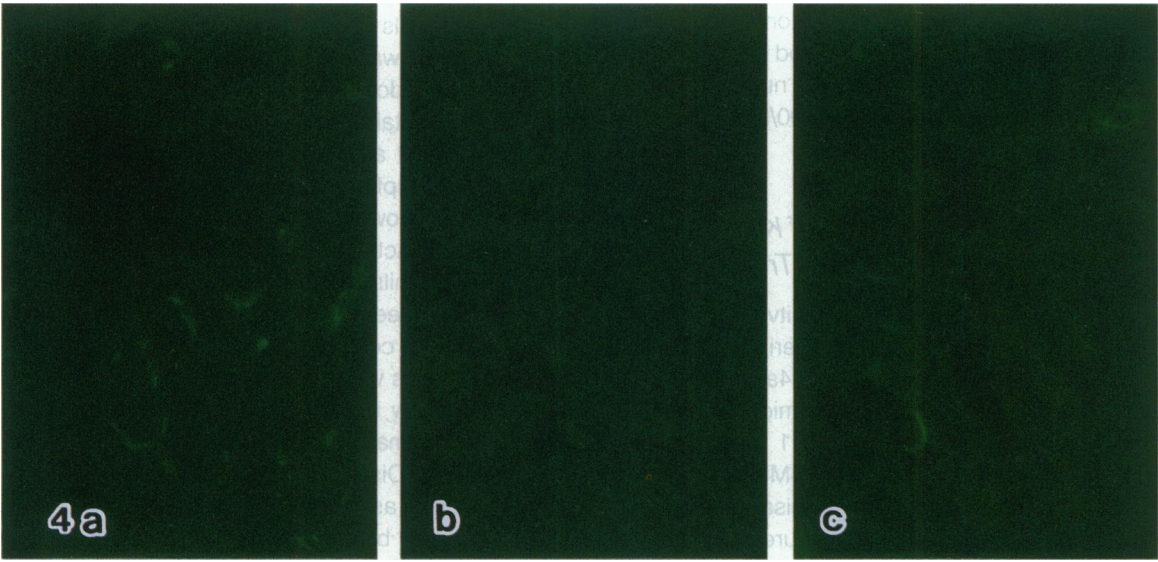
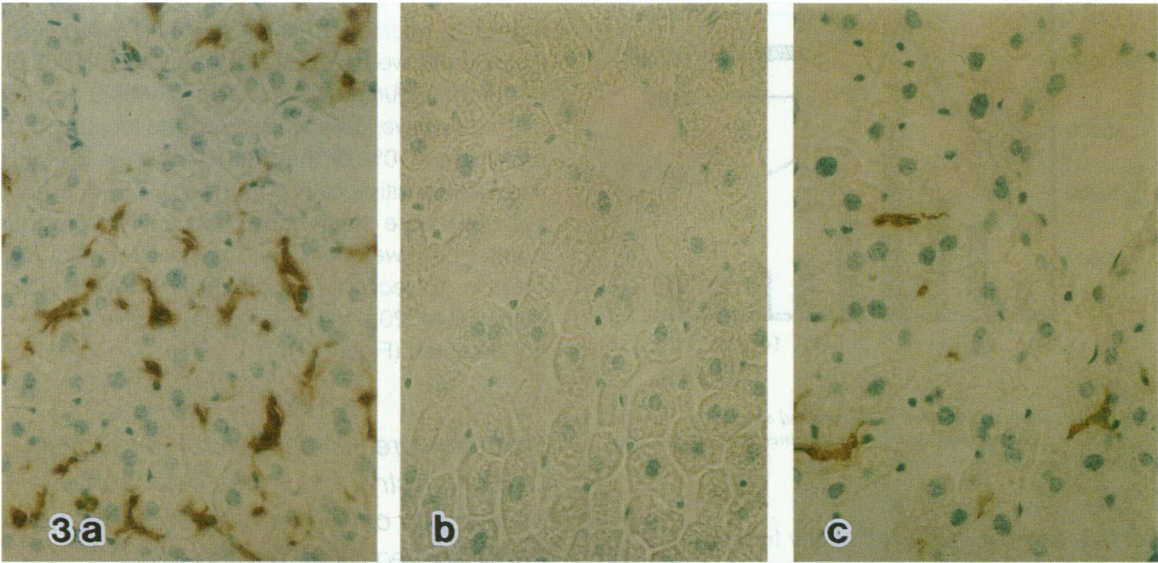
In normal untreated mice, BM8-positive Kupffer cells were found predominantly in the peripheral zone of the hepatic lobules (Figures 3a and 4a). Kupffer cells were strongly positive for histochemical staining for acid phosphatase (Figure 5a). At 1 day after liposome-entrapped MDP injection, BM8-positive and acid-phosphatase-positive cells disappeared and were not detected until day 4 (Figures 3b, 4b, and 5b). The numbers of BM8-positive and acid-phosphatase-positive cells started to increase from 5 days (Figures 3c, 4c, and 5c), reaching a plateau after 14 days (Figure 6). The distribution of the BM8-positive macrophages was rather irregular until 10 days, but they became larger and increased the intensity of acid phosphatase reactivity. Throughout the observation, ER-MP12-positive cells were not detectable in the liver. Although the numbers of ER-MP20- and ER-MP58-positive cells were small in untreated mice (Figure 7a), these macrophage precursor cells increased abruptly at 2 and 3 days, occasionally forming colonies in the liver (Figure 7b). Both ER-MP20-positive and ER-MP58-positive cells were mostly round (Figure 7, b and c). Immunohistochemical double staining demonstrated that the percentage of ER-MP58 and ER-MP20 double-positive cells in the total numbers of ER-MP58- and ER-

MP20-positive cells was 35% on 3 days followed by a gradual decrease. Almost all of the precursors in the colonies were doubly stained with ER-MP58 and ER-MP20 (Figure 8a). At 5 days, ER-MP20 and BM8 double-positive cells appeared and occupied approximately 10% of the total number of ER-MP20- and BM8-positive cells (Figure 8b). ER-MP20-positive cells were small and round and BM8-positive Kupffer cells were large and possessed many cytoplasmic projections (Figure 9). However, after 7 days, ER-MP20 and BM8 double-positive cells were not detected (Figure 10).

Ultrastructure, Ultrastructural Peroxidase Cytochemistry, and Immunoelectron Microscopy of Kupffer Cells in Liposome-Encapsulated MDP-Treated Mice

In Kupffer cells from untreated normal mice, peroxidase activity was localized in the nuclear envelope and rough endoplasmic reticulum. Kupffer cells were hardly detectable for 3 days after liposome-entrapped MDP administration, except for a few degenerative Kupffer cells containing a large amount of liposomes. However, the sinusoidal structure was otherwise intact. In the sinusoidal lumen, monocytes and neutrophils with peroxidase-positive granules were often seen. Besides, a few small immature mononuclear cells devoid of peroxidase activity in the organelles were present (Figure 11a). From 1 to 3 days, a few monocytes and small macrophages ingesting a small amount of liposomes were found in the space of Disse. In the sinusoid and the space of Disse as well as between hepatocytes, we detected a few round, blastic cells with abundant polyribosomes, round nuclei, and poorly developed cytoplasmic organelles that were all peroxidase negative (Figure 11b). From 5 days, macrophages with weak peroxidase activity in the nuclear envelope and rough endoplasmic reticulum adhered to the sinusoidal endothelial cells (Figure 11c). A few promonocytes and monoblasts with peroxidase activity in the nuclear envelope, rough endoplasmic reticulum, granules, and Golgi apparatus were observed. Peroxidase activity in the Kupffer cells became distinct, followed by enlargement and the development of intracellular organelles (Figure 11d).

Immunoelectron microscopically, reaction products by incubation with ER-MP58, ER-MP20, and BM8 were localized on the cell membrane. Ultrastructural features of ER-MP58-positive cells were compatible with those of monoblasts, promonocytes (Figure 12a), or more immature cells, sometimes



containing a few small granules. They occasionally formed colonies and showed mitotic figures (Figure 12b). ER-MP20-positive cells showed ultrastructural features of promonocytes, monocytes, and small macrophages. BM8-positive cells were large mature macrophages as well as small immature ones in ultrastructure.

Proliferative Potential of Kupffer Cells and Macrophage Precursors in Liposome-Encapsulated MDP-Treated Mice

To examine proliferative potential of Kupffer cells and their precursors, [³H]thymidine was given to mice at various times after liposome-entrapped MDP injection. In untreated mice, the ratio of [³H]thymidine-labeled cells to BM8-positive Kupffer cells was low and there were no labeled ER-MP20-positive or ER-MP58-positive cells in the liver. In mice given liposome-entrapped MDP, the increase of [³H]thymidine-labeled ER-MP58-positive cells was marked at 3 days (Figure 13a). At 5 days, the percentage of labeled cells in the total BM8-positive cells began to increase, reaching a maximum at 7 days (Figure 13b). The number of proliferating BM8-positive Kupffer cells returned to the normal range at 21 days (Figure 14).

Kinetics of Macrophages and Their Precursors

In contrast to the absence of [³H]thymidine labeling in ER-MP58- or ER-MP20-positive precursor cells in the liver of unmanipulated mice, approximately 5% of ER-MP58- and ER-MP20-positive precursor cells in the bone marrow were labeled with [³H]thymidine. In mice injected with liposome-entrapped MDP and [³H]thymidine simultaneously, therefore, only ER-MP20- or ER-MP58-positive cells in bone marrow were labeled and transferred to the peripheral blood and then to the liver. The ratios of ER-MP58- or ER-MP20-positive cells labeled with [³H]thymidine in the peripheral blood were high, reaching approximately 20 to 30% at 3 days (Figure 15a). The percentage of labeled cells among the ER-MP58- or ER-MP20-positive cells in the liver increased at 2 and 3 days but not by more than 4%. Cells labeled with

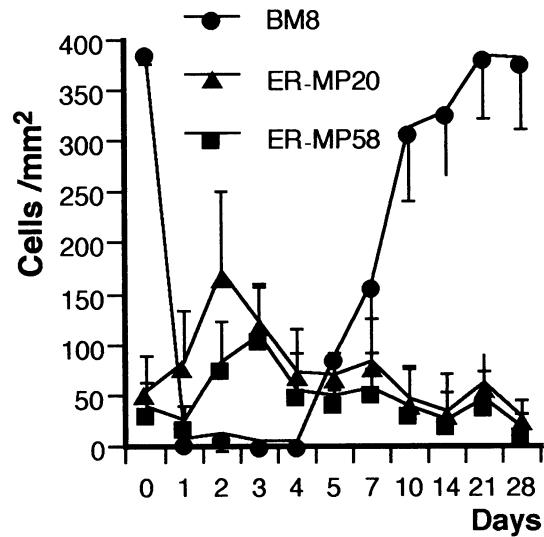


Figure 6. Changes in numbers of BM8-positive Kupffer cells and ER-MP20- and ER-MP58-positive precursors in the liver after the administration of liposome-entrapped MDP. Data are expressed as mean \pm SD.

[³H]thymidine among repopulating BM8-positive Kupffer cells were undetectable up to 7 days (Figure 15b).

In mice injected with [³H]thymidine at 2 days after liposome-entrapped MDP administration, proliferating cells both in the bone marrow and in the liver were labeled. The labeling indices of precursor cells in the bone marrow and the liver were much higher than those of the previous group of mice. A large number of ER-MP58-positive cells in the bone marrow were labeled first, and ER-MP58-positive cells in the peripheral blood reached the maximal level at 4 days (Figure 16a). The [³H]thymidine labeling rate of ER-MP58-positive cells in the liver increased apparently up to 30% at 3 days. BM8-positive cells were labeled with [³H]thymidine at 5 and 7 days (Figure 16, b and c), indicating that ER-MP58-positive cells differentiated into Kupffer cells.

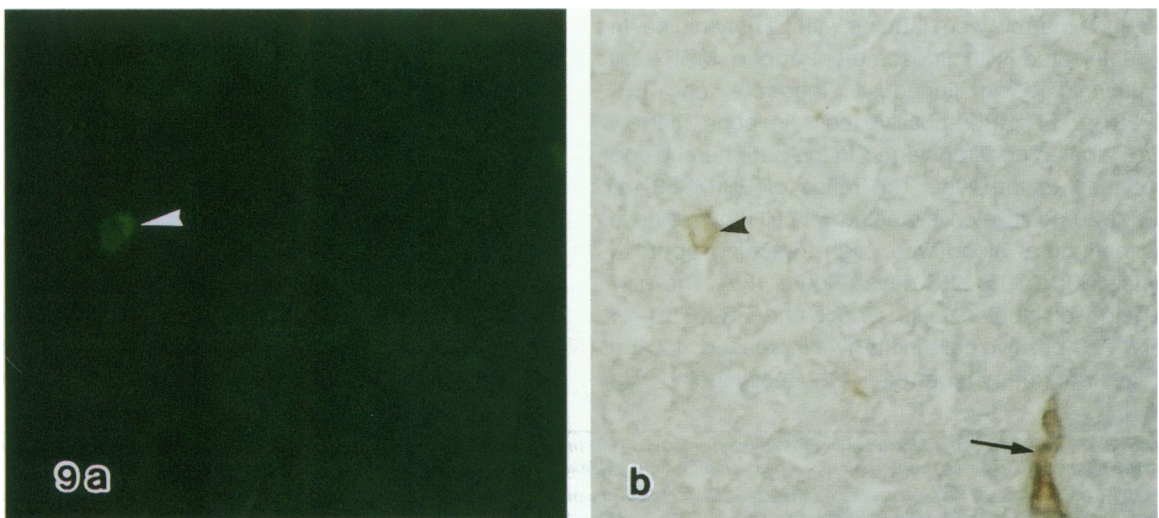
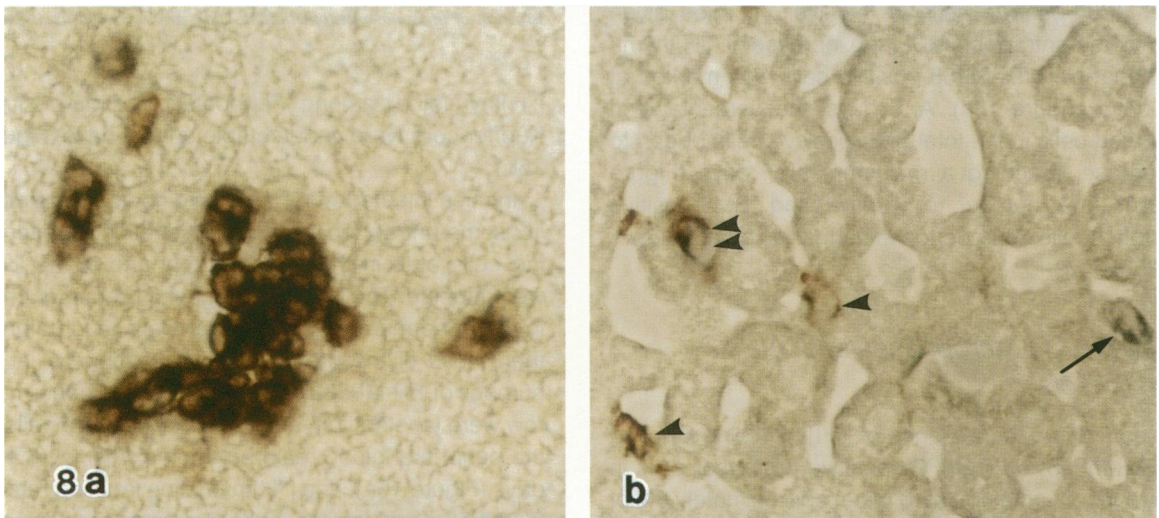
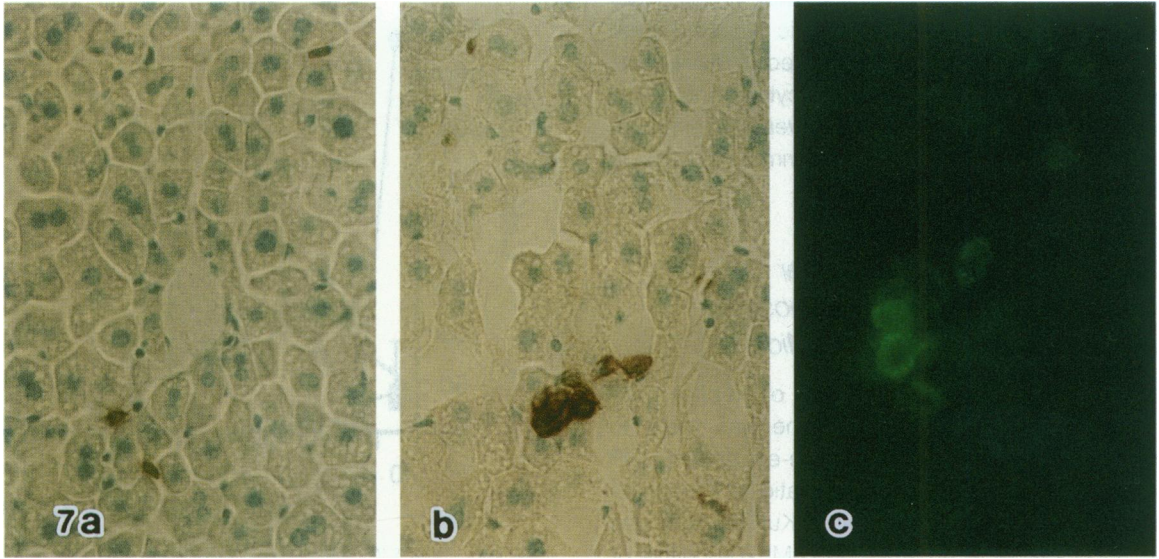
Changes in the Number of Repopulating Kupffer Cells after Daily Administration of Recombinant M-CSF

After liposome-entrapped MDP injection, there were no significant differences in the numbers and proliferative capacity of ER-MP20- and ER-MP58-positive

Figure 3. Disappearance and repopulation of BM8-positive Kupffer cells in the liver after the administration of liposome-entrapped MDP. Immunohistochemistry was performed using anti-macrophage monoclonal antibody BM8. a: Control. b: Day 3. c: Day 5. Magnification, $\times 400$.

Figure 4. Disappearance and repopulation of BM8-positive Kupffer cells in the liver after the administration of liposome-entrapped MDP. Immunofluorescent microscopy using BM8. a: Control. b: Day 3. c: Day 5. Magnification, $\times 400$.

Figure 5. Disappearance and repopulation of acid-phosphatase-positive cells (red) in the liver after the administration of liposome-entrapped MDP, using acid phosphatase histochemistry. a: Control. b: Day 3. c: Day 5. Small cells (arrowheads) are weakly positive for acid phosphatase. Magnification, $\times 400$.



cells in the liver between the M-CSF-treated and untreated mice. The number (Figure 17a) of repopulating BM8-positive Kupffer cells in M-CSF-treated mice was significantly larger than that in untreated mice at 5 and 7 days. However, their proliferative capacity was variable between the two groups of mice (Figure 17b), and the period of Kupffer cell depletion was not decreased by M-CSF.

Expression of M-CSF mRNA in the Liver of Liposome-Encapsulated MDP-Injected Mice

M-CSF mRNA was detected in the livers of normal and MDP-treated mice. At 2, 12, and 24 hours after liposome-entrapped MDP injection, mRNA expression was amplified (Figure 18a). At 24 hours, M-CSF mRNA was detected in the hepatocyte fraction but not in the MNC fraction of the liver (Figure 18b). IL-1 α mRNA was detected only at 2 hours after injection (data not shown). The expression of IL-3 and GM-CSF mRNA was not detectable.

Discussion

This study demonstrated that Kupffer cells were selectively eliminated in the mouse liver by injecting liposome-entrapped MDP and that they repopulated within 14 days. This finding is almost compatible with the previous observation that Kupffer cells completely repopulate in rats 16 days after depletion.¹³

Kupffer cells started to repopulate 5 days after liposome-entrapped MDP administration. In the early stage of their repopulation, small cells with immature ultrastructural features appeared and proliferated. They were positive for BM8 and weakly positive for acid phosphatase but devoid of peroxidase activity in the rough endoplasmic reticulum, the nuclear envelope, or granules, indicating that they were neither monocytes nor resident macrophages. These small immature macrophages became mature and developed peroxidase activity in the nuclear envelope and rough endoplasmic reticulum as well as acid phosphatase activity over several days. Similar immature

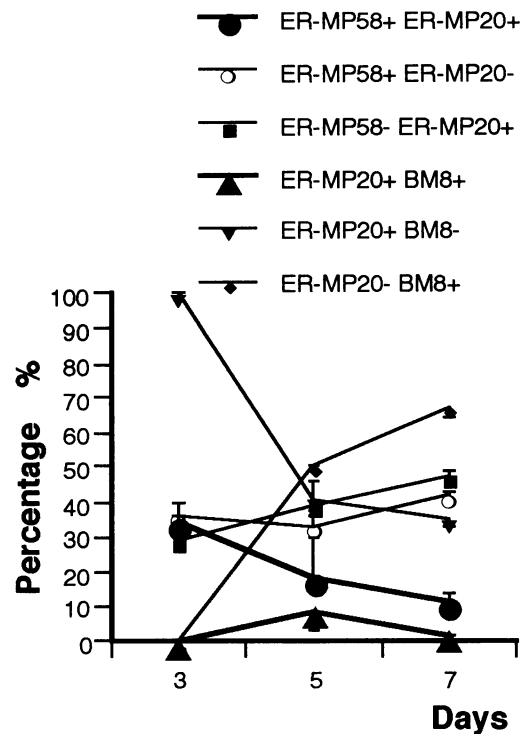


Figure 10. Changes in the immunophenotype of macrophages and their precursors in the liver after administration of liposome-entrapped MDP. Data are expressed as mean \pm SD.

macrophages reportedly develop and differentiate into resident macrophages in the fetal hematopoietic organs, and we designated these cells as primitive/fetal macrophages.^{34,35} The small immature macrophages found in this study and the primitive/fetal macrophages in the fetal hematopoietic organs share common features not only in morphology but also in having a high proliferative capacity. Small macrophages have also been detected in the regenerating rat liver⁶ and in the liver after lipopolysaccharide injection³⁶ and are regarded as precursors of Kupffer cells. In our Kupffer-cell-depleted model, the small macrophages appearing in the liver were considered to be direct precursors of repopulating Kupffer cells.

Colony-forming assays have demonstrated low concentrations of hematopoietic stem cells in the

Figure 7. a: There are only a few ER-MP58-positive cells in the liver of a control mouse. Immunohistochemistry using ER-MP58; magnification, $\times 600$. b: The numbers of ER-MP58-positive cells increased and occasionally formed colonies at 2 days after the administration of liposome-entrapped MDP. Immunohistochemistry using ER-MP58; magnification, $\times 600$. c: ER-MP20-positive cells also formed colonies at 2 days after the administration of liposome-entrapped MDP. Immunofluorescence microscopy using ER-MP20; magnification, $\times 600$.

Figure 8. a: The numbers of ER-MP58 and ER-MP20 double-positive cells (dark brown) increased, and they formed colonies at 3 days after the administration of liposome-entrapped MDP. Immunohistochemical double staining; magnification, $\times 600$. b: At 5 days, ER-MP20 and BM8 double-positive cells (double arrowheads, dark brown) as well as ER-MP20-positive and BM8-negative cells (arrow, blue) and ER-MP20-negative and BM8-positive cells (arrowhead, brown) were detected in the liver. Immunohistochemical double staining; magnification, $\times 600$.

Figure 9. a: A round cell is demonstrated to be ER-MP20 positive by immunofluorescence (arrowhead) at 5 days after administration liposome-entrapped MDP. Magnification, $\times 600$. b: Round and polygonal BM8-positive cells (arrowhead and arrow). Immunohistochemical staining using BM8 in the same section as a; magnification, $\times 600$. The round BM8-positive cell (black arrowhead) is demonstrated also to be ER-MP20 positive by immunofluorescence (white arrowhead).

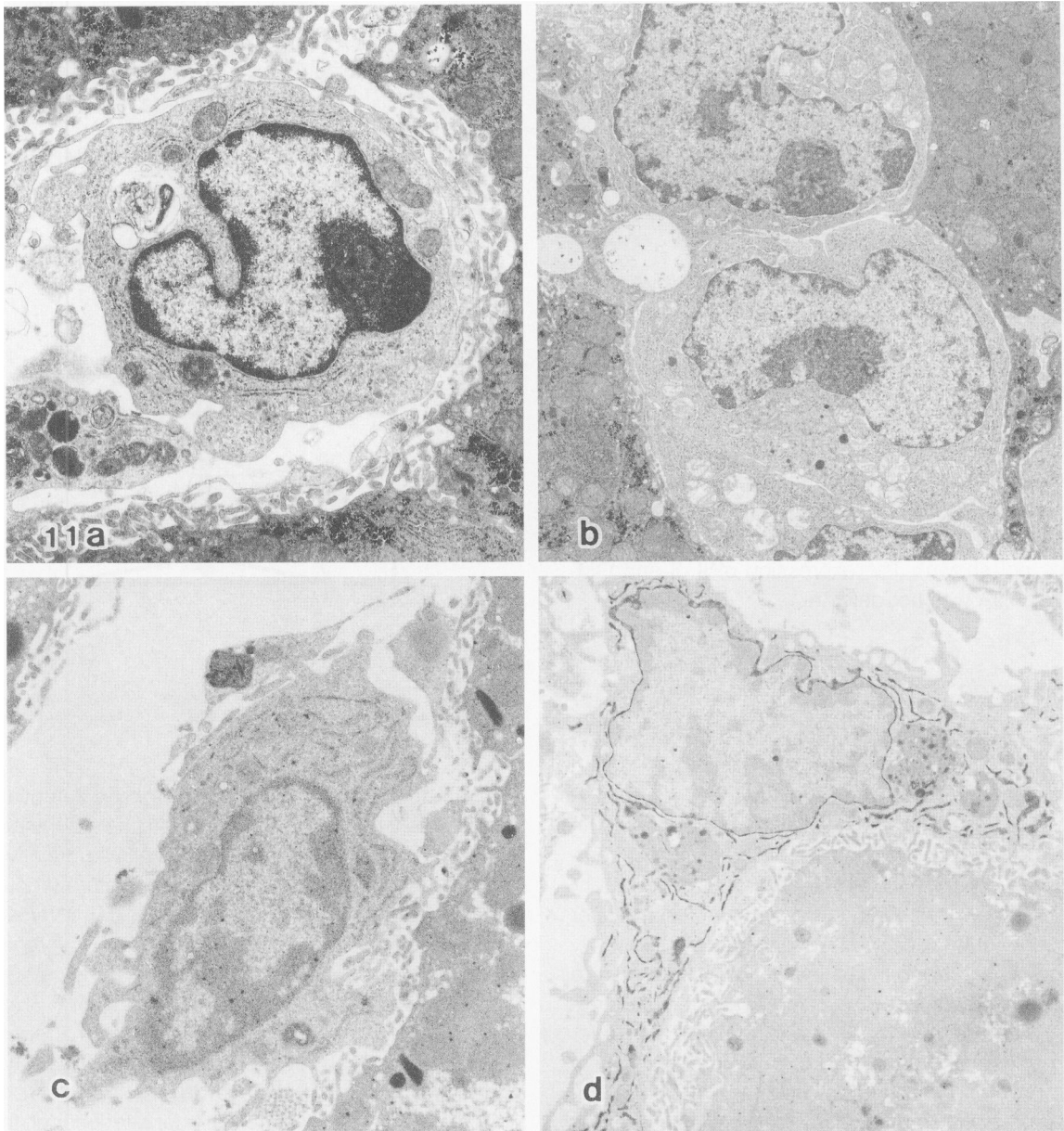


Figure 11. Ultrastructural peroxidase cytochemistry of repopulating macrophages. **a:** Immature round cell observed at 2 days had no peroxidase activity in the organelles. Magnification, $\times 6000$. **b:** At 2 days, blastic cells with or without a few peroxidase-positive granules appeared. Magnification, $\times 6000$. **c:** At 7 days after administration, macrophages with weak peroxidase activity in the nuclear envelope and rough endoplasmic reticulum were found. Magnification, $\times 6000$. **d:** At 14 days, peroxidase activity in Kupffer cells became distinct within days, followed by the enlargement and development of intracellular organelles. Magnification, $\times 6000$.

adult mouse liver, and their number increased after partial hepatectomy.^{37,38} Hematopoietic stem cells have been found in the adult mouse liver based on the results of liver cell transplantation.³⁹ These hematopoietic cells from the liver formed colonies *in vivo* and *in vitro* and reconstituted bone marrow of lethally irradiated recipient mice for at least several months.³⁹ However, hematopoietic progenitors in the adult mouse liver have not been found *in situ*. To detect macrophage precursors, we used monoclo-

nal antibodies raised against murine macrophage precursors.^{25,26} ER-MP12 is similar to CD34 with regard to the high level of expression by early hematopoietic cells. ER-MP58 reacts mainly with cells at the level of colony forming units of granulocytes and macrophages (CSU-GM) responsive to M-CSF and colony forming units of macrophages (CFU-M). ER-MP20 is a typical marker of intermediate stages of bone-marrow-derived macrophage maturation including monocytes (Figure 1). In this study, ER-

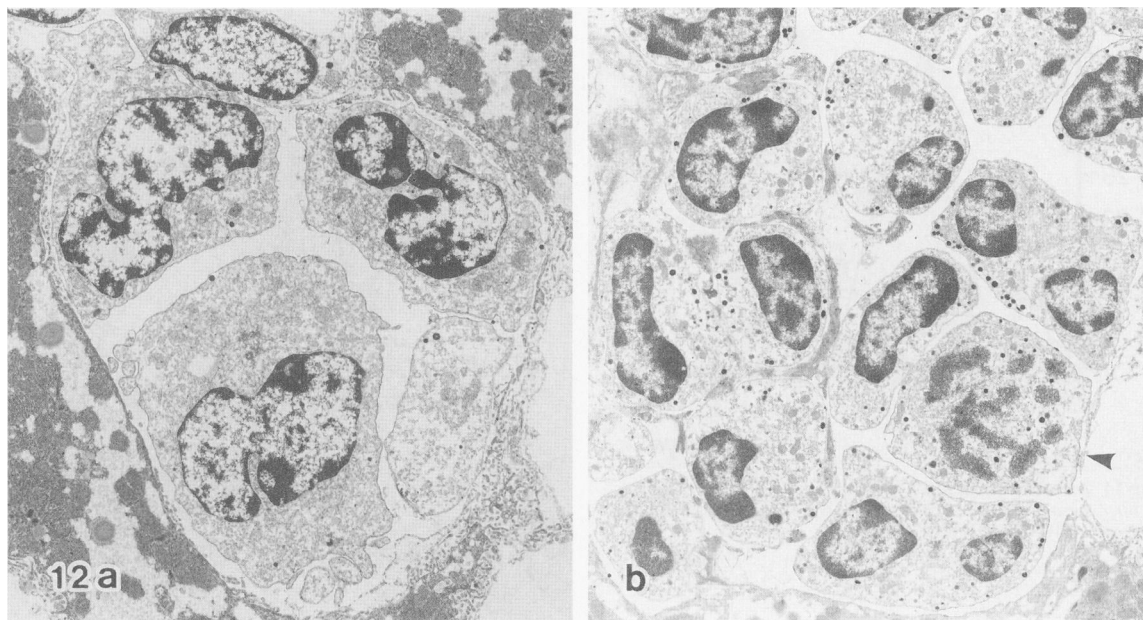


Figure 12. Immunoelectron microscopy using ER-MP58. **a:** Reaction products for ER-MP58 are present on the cell membrane of immature cells forming a colony. They contain a few tiny granules. Magnification, $\times 4000$. **b:** A mitotic figure (arrowhead) is seen in a colony. Magnification, $\times 2000$.

MP12-positive cells were not detectable. However, there were ER-MP58- and ER-MP20-positive cells in the livers of normal mice, and the present immunoelectron microscopic observation confirmed the reactivity of these monoclonal antibodies to macrophages and their precursors. During Kupffer cell

depletion, the numbers of ER-MP58- and ER-MP20-positive cells increased approximately threefold compared with those in normal mice. Autoradiography revealed that ER-MP58-positive precursor cells constituted a highly proliferating population in the liver during the period of Kupffer cell depletion,

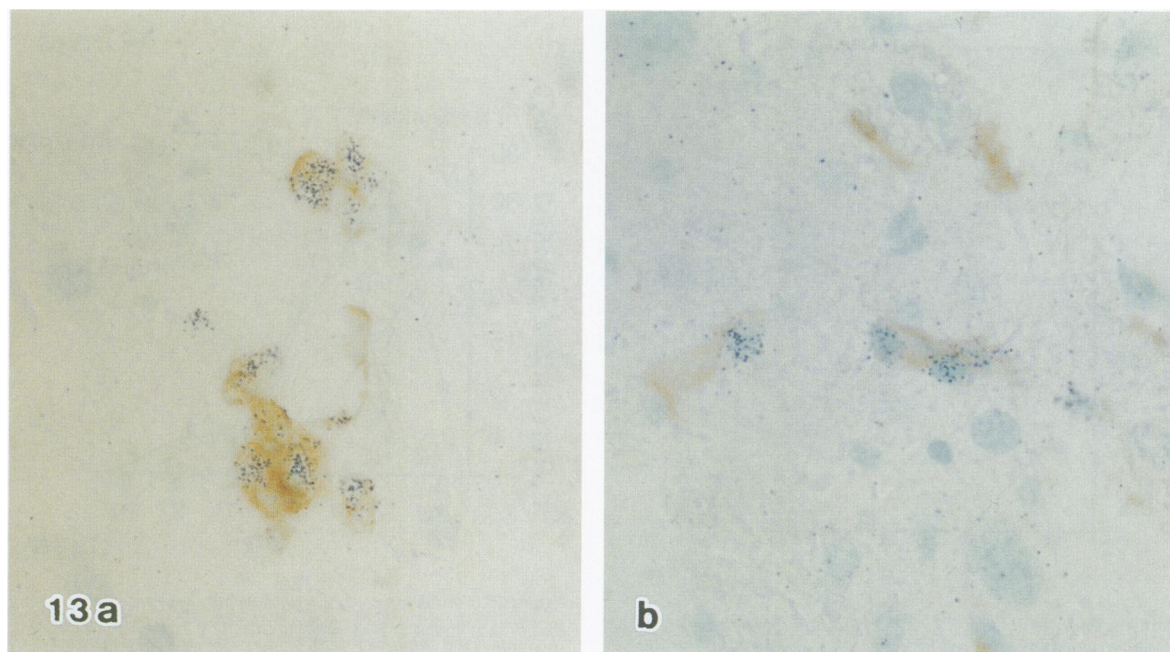


Figure 13. Combined immunohistochemistry and ^3H -thymidine autoradiography. **a:** ER-MP58-positive cells contain many grains on their nuclei at 5 days after administration of liposome-entrapped MDP. Magnification, $\times 600$. **b:** Repopulating BM8-positive Kupffer cells also show a high labeling rate at 5 days. Magnification, $\times 600$.

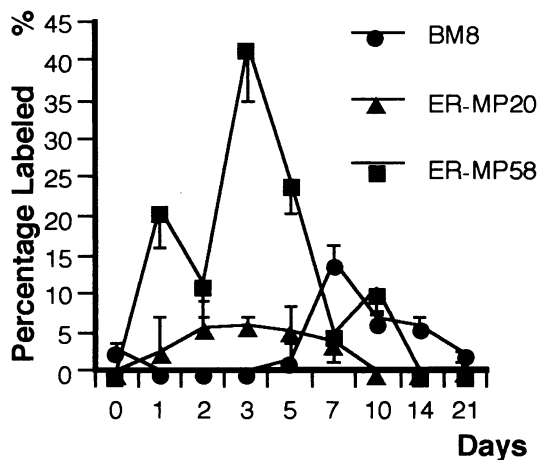


Figure 14. The proliferation indices of Kupffer cells and their precursor cells after the administration of liposome-entrapped MDP. Data are expressed as mean \pm SD.

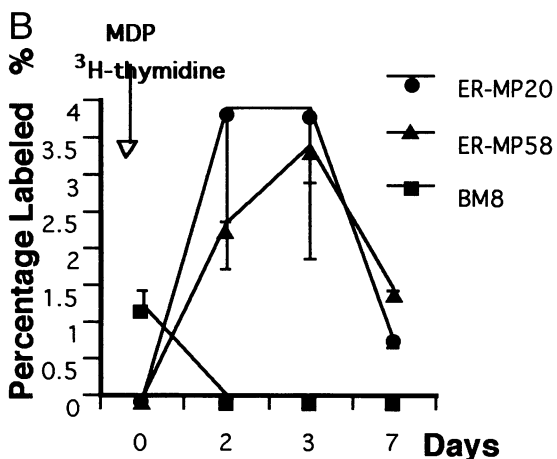
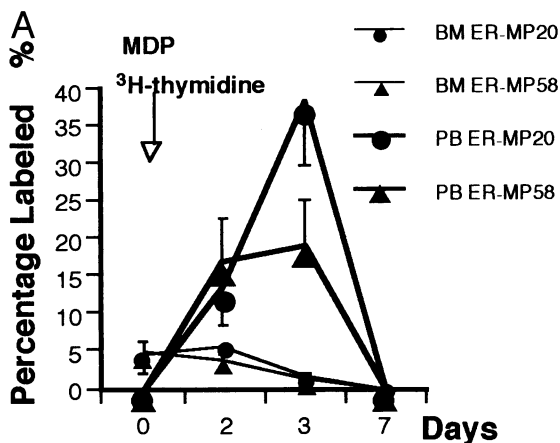
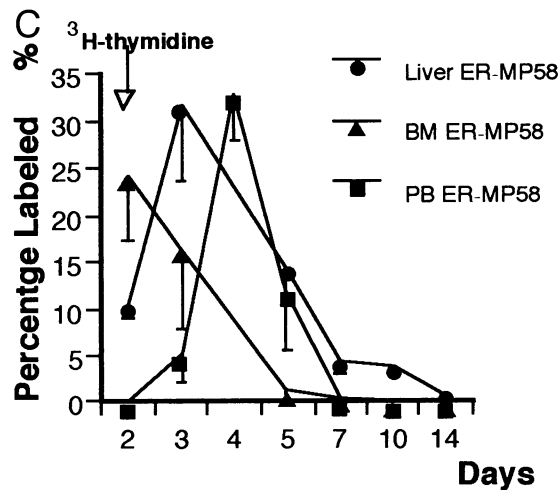
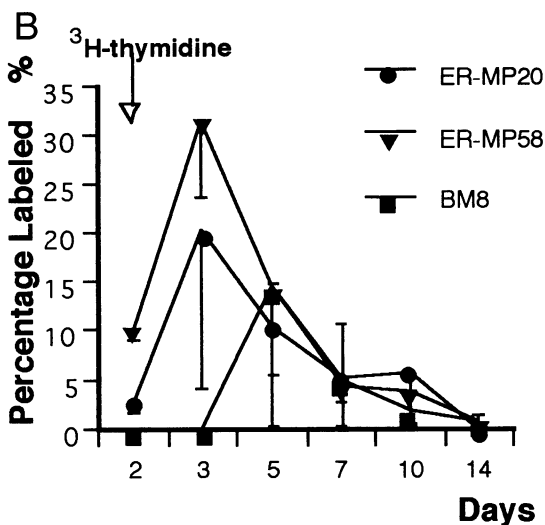
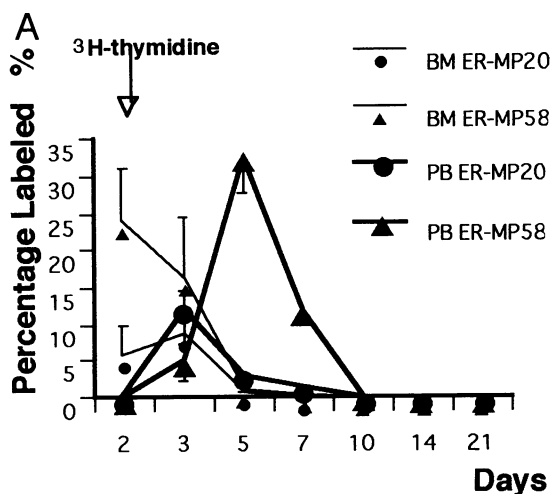


Figure 15. Changes in the ^3H -thymidine labeling rates of Kupffer cells and macrophage precursor cells after the simultaneous administration of liposome-entrapped MDP and ^3H -thymidine. a: The labeling rates of ER-MP20- and ER-MP58-positive cells in bone marrow (BM) and peripheral blood (PB). b: The labeling rate of Kupffer cells in the liver. Data are expressed as mean \pm SD.

Figure 16. Changes in the ^3H -thymidine labeling rates of macrophage precursor cells and Kupffer cells after labeling with ^3H -thymidine at 2 days after the administration of liposome-entrapped MDP. a: The labeling rates of cells in bone marrow and peripheral blood. b: The labeling rate of cells in the liver. c: The labeling rates of ER-MP58-positive cells in bone marrow (BM), peripheral blood (PB), and liver. Data are expressed as mean \pm SD.

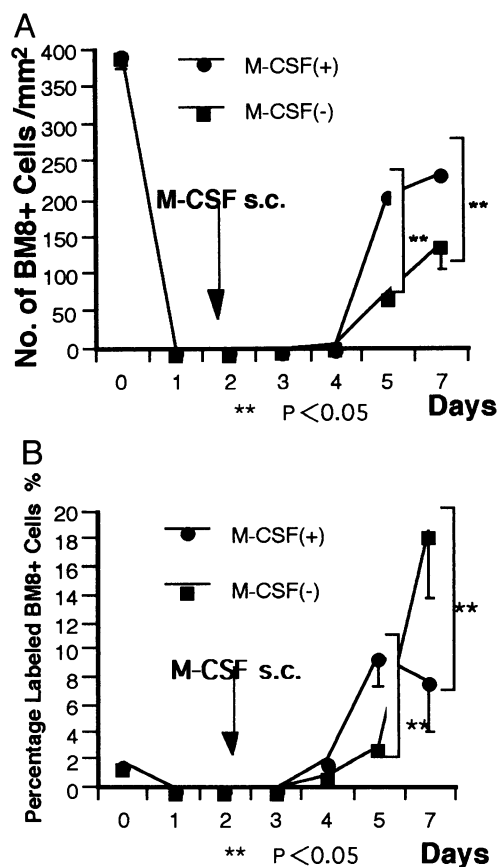


Figure 17. a: Numbers of BM8-positive cells in the livers of M-CSF-treated and untreated mice after the administration of liposome-entrapped MDP. b: Proliferative capacity of BM8-positive cells in the livers of M-CSF-treated and untreated mice after the administration of liposome-entrapped MDP. Data are expressed as mean \pm SD.

whereas they did not proliferate in an unstimulated condition. These results suggested that these precursors represent steady components of the liver

that are essentially inactive until stimulated to proliferate.

A question arises as to whether or not the macrophage precursors in the liver serve as progenitors of repopulating Kupffer cells. Combining the results of immunohistochemical double staining and [³H]thymidine autoradiography, ER-MP58-positive precursor cells proliferated and differentiated into ER-MP58 and ER-MP20 double-positive, ER-MP20-positive, and ER-MP20 and BM8 double-positive cells and finally into BM8-positive Kupffer cells. The BM8-positive Kupffer cells also proliferate, especially during the early stage of repopulation. These results indicated that ER-MP58-positive cells play an important role in the repopulation of Kupffer cells after liposome-entrapped MDP administration. However, the possibility that ER-MP58- and ER-MP20-positive cells migrate from the bone marrow cannot be excluded.

In the normal untreated mouse liver, labeling indices of ER-MP58- and ER-MP20-positive cells were almost 0%. Therefore, the simultaneous administration of [³H]thymidine and liposome-entrapped MDP can selectively label precursor cells in bone marrow. This experiment demonstrated that ER-MP58-positive cells in the bone marrow migrate into the peripheral blood and reach to the liver after an injection of liposome-entrapped MDP. However, differentiation from bone-marrow-derived precursor cells into BM8-positive cells was not detected in the liver. In contrast, pulse labeling performed 2 days after liposome-entrapped MDP injection labeled precursors in the bone marrow and in the liver. ER-MP58-positive cells in the liver proliferated and some of them differentiated into BM8-positive cells. These results suggested that there are macrophage precursor

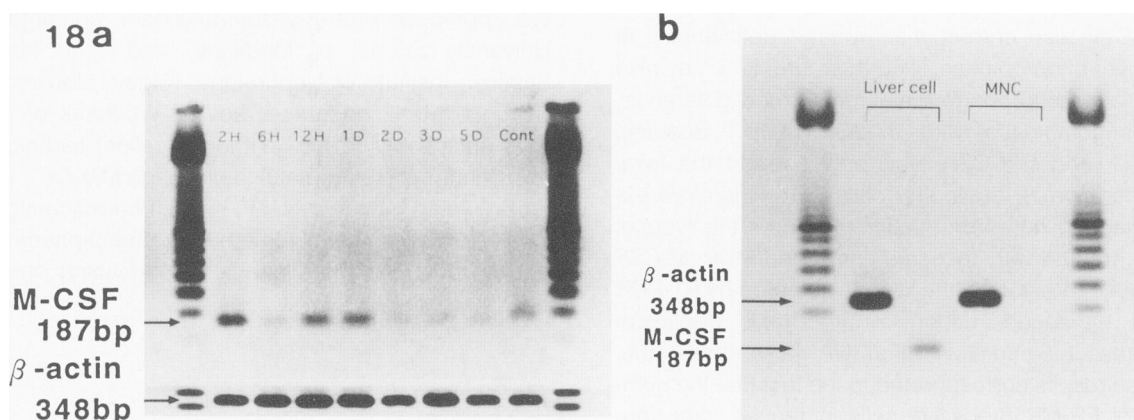


Figure 18. Expression of M-CSF mRNA in the liver detected by RT-PCR. a: M-CSF mRNA expression is enhanced at 2, 12, and 24 hours after the administration of liposome-entrapped MDP. b: M-CSF mRNA expression is detected in the liver cell fraction but not in that of the MNCs at 24 hours.

pools in the liver of normal mice and that these precursor cells proliferate and participate in the repopulating process of Kupffer cells after their depletion. Thus, macrophage precursors in the liver after injection of liposome-entrapped MDP were composed of bone-marrow-derived and intrahepatic proliferating populations. The significance and the relationship between these two precursor populations should be clarified by further investigation.

In contrast to previous studies, the increases of neutrophils and monocytes were remarkable in mice after liposome-encapsulated MDP administration. The mechanism as to the induction of leukocytosis is unknown. Considering the appearance of ER-MP58-positive cells in peripheral blood, substances released from destroyed macrophages may have stimulated the release of leukocytes including myeloid precursors from bone marrow. It is postulated that Kupffer cells phagocytize neutrophils undergoing apoptosis.⁴⁰ Marked leukocytosis may result from a dysfunction of the leukocyte clearance system due to the depletion of Kupffer cells.

Several growth factors modulate the differentiation and maturation of macrophage precursors.^{18,41-43} The liver is a hematopoietic organ during fetal development, and M-CSF is detected in the fetal liver.²³ In the adult rat liver, focal hematopoiesis is induced by the administration of glucan, which increases the production of M-CSF and GM-CSF in the liver.⁴⁴ Osteopetrosis (*op/op*) mice lacking functional activity of M-CSF due to a mutation in the coding region of the M-CSF gene itself^{45,46} are characterized by an absence of monocytes in the peripheral blood and a disturbance in their differentiation into macrophages.^{19,20,45-48} The administration of M-CSF to *op/op* mice corrects the reduction of Kupffer cells.¹⁸ Thus, the major population of Kupffer cells is regarded as M-CSF-dependent macrophages. However, daily administrations of recombinant murine GM-CSF also correct macrophage deficiencies in the liver of *op/op* mice.⁴⁹ Furthermore, IL-3 may also regulate macrophage development and differentiation in combination with GM-CSF *in vitro*.⁴⁶ Besides, M-CSF and GM-CSF reportedly support the local proliferation of rat Kupffer cells.⁵⁰ We therefore examined the *in loco* production of CSFs in the livers of mice treated with liposome-entrapped MDP. M-CSF mRNA expression in the liver as detected by RT-PCR was enhanced during Kupffer cell depletion, whereas IL-3 and GM-CSF mRNA was undetectable. These results corresponded to the fact that the number of ER-MP58-positive cells increased after liposome-encapsulated MDP injection because they are M-CSF responsive.²⁶ Although a significant differ-

ence was not detected in the proliferative potential of ER-MP58-positive precursor cells in the liver between M-CSF-treated and untreated mice, the number and the proliferative potential of repopulating BM8-positive Kupffer cells was significantly larger in M-CSF-treated mice than those in untreated mice. We also confirmed marked proliferation of small immature Kupffer cells in *op/op* mice after M-CSF administration.²⁰ Taken all together, it is suggested that M-CSF promotes the differentiation and proliferation of repopulating immature Kupffer cells and their precursors.

Hepatocytes and sinusoidal cells produce M-CSF and GM-CSF to regulate the proliferation, differentiation, and maturation of Kupffer cells.^{22,38} These CSFs are also secreted by Kupffer cells themselves. To clarify the source of M-CSF production, we fractionated the liver tissue and detected M-CSF mRNA expression in the hepatocyte but not in the MNC fraction. Because Kupffer cells were completely eliminated by liposome-entrapped MDP for 4 days, hepatocytes are responsible for the enhanced expression of M-CSF mRNA at 12 and 24 hours. The augmented M-CSF mRNA expression at 2 hours as well as the temporary expression of IL-1 mRNA may reflect a Kupffer cell activation by liposome phagocytosis before they are destroyed by liposome-entrapped MDP.

In summary, after depleting Kupffer cells by injecting liposome-entrapped MDP, macrophage precursor cells increased and proliferated in the liver and differentiated into Kupffer cells. The liver provides a microenvironment for the differentiation, proliferation, and maturation of Kupffer cells and their precursors by the local production of M-CSF.

Acknowledgments

We appreciate Prof. Kiyoshi Takahashi, Kumamoto University School of Medicine, and Prof. Fujio Shimizu, Institute of Nephrology, Niigata University School of Medicine for their advice. We thank Mr. K. Sato and S. Momozaki for their excellent technical assistance. We are grateful to Morinaga Milk Co. Ltd. for providing human rM-CSF, Kissei Pharmaceutical Co. for supplying dichloromethylene diphosphonate, and Nippon Fine Chemical Co. for providing phosphatidylcholine.

References

1. van Furth R, Disselhoff-den Dulk MMC, Sluiter W, van Dissel JT: New perspectives on the kinetics of mono-

- nuclear phagocytes. Mononuclear Phagocytes: Characteristics: Physiology and Function. Edited by R van Furth. Dordrecht, The Netherlands, Martinus Nijhoff, 1985, pp 201–210
- Wacker H-H, Radzun HJ, Parwaresch MR: Kinetics of Kupffer cells as shown by parabiosis and combined autoradiographic/immunohistochemical analysis. *Virchows Arch (Cell Pathol)* 1986, 51:71–78
 - Bouwens L, Wisse E: Proliferation, kinetics, and fate of monocytes in rat liver during a zymosan-induced inflammation. *J Leukocyte Biol* 1985, 37:531–543
 - Kojima M: Macrophages, reticuloendothelial system, and mononuclear phagocyte system. *Recent Adv Res* 1976, 16:1–10
 - Widmann J-J, Fahimi HD: Proliferation of mononuclear phagocytes (Kupffer cells) and endothelial cells in regenerating rat liver: a light and electron microscopic study. *Am J Pathol* 1975, 80:349–366
 - Ukai K, Terashima K, Imai Y, Shinzawa H, Okuyama Y, Takahashi T, Ishikawa M: Proliferation kinetics of rat Kupffer cells after partial hepatectomy. *Acta Pathol Jpn* 1990, 40:623–634
 - Deimann W, Fahimi H: Hepatic granulomas induced by glucan: an ultrastructural and peroxidase-cytochemical study. *Lab Invest* 1980, 43:172–181
 - Parwaresch MR, Wacker H-H: Origin and kinetics of resident tissue macrophages: parabiosis studies with radiolabelled leucocytes. *Cell Tissue Kinet* 1984, 17:25–39
 - Volkman A: Disparity in origin of mononuclear phagocyte population. *J Reticuloendothel Soc* 1976, 19:249–268
 - Yamada M, Naito M, Takahashi K: Kupffer cell proliferation and glucan-induced granuloma-formation in mice depleted of blood monocytes by strontium-89. *J Leukocyte Biol* 1990, 47:195–205
 - Naito M, Takahashi K: The role of Kupffer cells in glucan-induced granuloma formation in the mouse liver depleted of blood monocytes by administration of strontium-89. *Lab Invest* 1991, 50:664–674
 - van Rooijen N, Kors N, Kraal G: The liposome-mediated macrophage: a suicide technique. *J Immunol Methods* 1989, 124:1–6
 - van Rooijen N, Kors N, van der Ende M, Dijkstra CD: Depletion and repopulation of macrophages in spleen and liver of rat after intravenous treatment with liposome-encapsulated dichloromethylene diphosphate. *Cell Tissue Res* 1990, 260:215–222
 - van Rooijen N, Kors N, Kraal G: Macrophage subset repopulation in the spleen: differential kinetics after liposome-mediated elimination. *J Leukocyte Biol* 1989, 45:97–104
 - van Rooijen N, van Nieuwenmegen R: Elimination of phagocytic cells in the spleen after intravenous injection of liposome-encapsulated dichloromethylene diphosphate. *Cell Tissue Res* 1984, 238:355–358
 - Delemarre FG, Kors N, Kraal G, van Rooijen N: Repopulation of macrophages in popliteal lymph nodes of mice after liposome-mediated depletion. *J Leukocyte Biol* 1990, 47:251–257
 - van Rooijen N, Sanders A: Liposome mediated depletion of macrophages: mechanism of action, preparation of liposomes, and applications. *J Immunol Methods* 1994, 174:83–93
 - Morioka Y, Naito M, Sato T, Takahashi K: Immunophenotypic and ultrastructural heterogeneity of macrophage differentiation in bone marrow and fetal hematopoiesis *in vitro* and *in vivo*. *J Leukocyte Biol* 1994, 55:642–651
 - Naito M, Hayashi S-I, Yoshida H, Takahashi K: Abnormal differentiation of tissue macrophage populations in "osteopetrosis" (*op*) mice defective in the production of macrophage colony-stimulating factor (M-CSF) or CSF-1. *Am J Pathol* 1991, 139:657–667
 - Takahashi K, Naito M, Umeda S, Shultz LD: The role of macrophage colony-stimulating factor in hepatic glucan-induced granuloma formation in the osteopetrosis mutant mouse defective in the production of macrophage colony-stimulating factor. *Am J Pathol* 1994, 144:1381–1392
 - Honda Y, Takahashi K, Naito M, Fijiyama S: The role of colony-stimulating factor in the differentiation and proliferation of Kupffer cells in the liver of protein-deprived mice. *Lab Invest* 1995, 72:696–706
 - Tsukui T, Kikuchi K, Sudo T, Sakamoto T, Sato N: Production of macrophage colony-stimulating factor by adult murine parenchymal liver cells (hepatocytes). *J Leukocyte Biol* 1992, 52:383–389
 - Azoulay M, Webb CG, Sachs L: Control of hematopoietic cell growth regulators during mouse fetal development. *Mol Cell Biol* 1987, 7:3361–3364
 - Kiwada H, Niimura H, Fujisaki Y: Application of synthetic alkyl glycosides vesicles as drug carrier. I. Preparation and physical properties. *Chem Pharmacol Bull* 1985, 33:753–759
 - Leenen PJM, Melis M, Slieker WAT, van Ewijk W: Murine macrophage precursor characterization. II. Monoclonal antibodies against macrophage precursor antigens. *Eur J Immunol* 1990, 20:27–34
 - Leenen PJM, de Bruijn MFTR, Voerman JSA, Campbell PA, van Ewijk W: Markers of mouse macrophage development detected by monoclonal antibodies. *J Immunol Methods* 1994, 176:5–19
 - Isobe S, Chen S-T, Nakane PK, Brown WR: Studies on translocation of immunoglobulins across intestinal epithelium. I. Improvements to study the peroxidase-labeled antibody method for application to study of human intestinal mucosa. *Acta Histochem Cytochem* 1977, 10:161–171
 - Higashi K, Naito M, Takeya M, Ando M, Araki S, Takahashi K: Ontogenic development, differentiation, and phenotypic expression of macrophages in fetal rat lungs. *J Leukocyte Biol* 1992, 51:444–454
 - Chilosi MD, Pizzolo G, Menestrina F, Iannucci AM, Bonetti F, Fiore-Donati L: Enzyme histochemistry on

- normal and pathologic paraffin-embedded lymphoid tissues. *Am J Clin Pathol* 1981, 76:729-736
30. Wisse E: Observation on the fine structure and peroxidase cytochemistry of normal rat liver Kupffer cells. *J Ultrastruct Res* 1974, 46:393-426
 31. Graham RC, Karnovsky MJ: The early stages of absorption of injected horseradish peroxidase in the proximal tubules of mouse kidney: ultrastructural cytochemistry by a new technique. *J Histochem Cytochem* 1966, 14:291-302
 32. Xiong H, Kawamura I, Takeaki N, Mitsuyama M: Cytokine gene expression in mice at an early stage of infection with various strains of *Listeria* spp differing in virulence. *Infect Immun* 1994, 62: 3649-3654
 33. Ohteki T, Seki S, Abo T, Kumaga T: Liver is possible site for the proliferation of abnormal CD3⁺4⁻8⁻ double-negative lymphocytes in autoimmune MRL-*lpr/lpr* mice. *J Exp Med* 1990, 172:7-12
 34. Takahashi K, Yamamura F, Naito M: Differentiation, maturation, and proliferation of macrophages in the mouse yolk sac: a light microscopic enzyme-cytochemical, immunohistochemical, and ultrastructural study. *J Leukocyte Biol* 1989, 45:87-96
 35. Naito M, Yamamura F, Nishikawa S: Development, differentiation, and maturation of fetal mouse yolk sac macrophages. *J Leukocyte Biol* 1989, 46:1-10
 36. van Bossuyt H, Wisse E: Structural changes produced in the rat liver by injection of lipopolysaccharide. *Cell Tissue Res* 1988, 251:205-214
 37. Hays EF, Golde DW, Hays DM: Hematopoietic stem cells in mouse liver. *Exp Hematol* 1976, 61:18-27
 38. Sakamoto T, Mabuchi A, Kuriya S, Sudo T, Aida T, Asan G: Production of granulocyte-macrophage colony-stimulating factor by adult murine parenchymal liver cells (hepatocytes). *Regul Immunol* 1991, 3:260-267
 39. Taniguchi H, Toyoshima T, Fukao K, Nakauchi H: Evidence of presence of hematopoietic stem cells in adult liver. *Transplant Proc* 1995, 27:196-199
 40. Sato T, Takahashi T, Shinzawa H, Arai S, Abe Y, Sendo F: Inhibition of *Corynebacterium parvum*-primed and lipopolysaccharide-induced hepatic necrosis in rats by selective depletion of neutrophils using a monoclonal antibody. *J Leukocyte Biol* 1993, 53:144-150
 41. Metcalf D: The molecular control of cell division, differentiation commitment, and maturation in haematopoietic cells. *Nature* 1989, 339:27-30
 42. Metcalf D, Nicola NA: The clonal proliferation of normal mouse hematopoietic cells: enhancement and suppression by colony stimulating factor combination. *Blood* 1992, 79:2861-2866
 43. Metcalf D, Nicola NA, Gough NM, Elliot G, McArthur G, Li M: Synergistic suppression: anomalous inhibition of the proliferation of factor-dependent hematopoietic cells by combination of two colony-stimulating factor. *Proc Natl Acad Sci USA* 1992, 89:2819-2823
 44. Deiman W, Fahimi HD: Induction of focal hematopoiesis in adult rat liver by glucan, a macrophage activator. *Lab Invest* 1980, 42:217-224
 45. Yoshida H, Hayashi SI, Kunisada T, Ogawa M, Nishikawa S, Okamura H: The murine mutation osteopetrosis is in the coding region of the macrophage colony stimulating factor gene. *Nature* 1990, 345:442-443
 46. Wiktor-Jedrzejczak W, Bartocci A, Ferrante AW Jr, Ahmed-Ansari A, Sel KW, Pollard TW, Stanley ER: Total absence of colony-stimulating factor in the macrophage-deficient osteopetrotic (*op/op*) mouse. *Proc Natl Acad Sci USA* 1990, 87:4828-4832
 47. Wiktor-Jedrzejczak W: *In vivo* role of macrophage growth factors as delineated using CSF-1 deficient *op/op* mouse. *Leukemia* 1993, 2:S117-121
 48. Nishikawa SI, Hayashi SI, Yoshida H, Naito M, Takahashi K, Shultz LD: A model mouse defective in M-CSF production: molecular biology and pathology of osteopetrosis mouse (*op/op*). *Dendritic Cells in Lymphoid Tissue*. Edited by Y Imai, JG Tew, ECM Hoefsmit. Amsterdam, Elsevier Science Publishers, 1991, pp 225-231
 49. Wiktor-Jedrzejczak W, Uravanowska E, Szperl M: Granulocyte-macrophage colony-stimulating factor corrects macrophage deficiencies, but not osteopetrosis, in the colony-stimulating factor 1-deficient *op/op* mouse. *Exp Hematol* 1992, 20:769
 50. Hoedemakers RMJ, Scherphof GL, Daemaen T: Proliferation of rat liver macrophages *in vitro*: influence of hemopoietic growth factors. *Hepatology* 1994, 19:666-674